Experimental Determination of the Hydrodynamic Parameters of an OWC

Thomas Kelly*, Thomas Dooley† and John V. Ringwood*
*Department of Electronic Engineering, Maynooth University, Co. Kildare, Ireland.
E-mail: thomas.e.kelly.2012@mumail.ie
E-mail: john.ringwood@eeng.nuim.ie
†Centre for Renewable Energy at Dundalk IT, Dundalk Institute of Technology, Dublin Rd., Dundalk, Ireland.
E-mail: thomas.dooley@dkit.ie

***Abstract*—A novel technique to measure the frequency-dependent hydrodynamic parameters of an oscillating water column (OWC) using tank testing is proposed. This technique arose from investigations into the effect on the power absorbed by OWCs of air compressibility in the chamber above the water column. Two models of an OWC were constructed for that investigation. For the first model, the volume of the air chamber above the water column was scaled geometrically by the factor to which the water column was scaled. For the second, the volume of the air chamber was scaled by the square of the factor to which the water column was scaled. The proposed technique to measure the hydrodynamic parameters, which eliminates the need for a forced-oscillation rig, uses these two OWC models, and relies on water column motion which takes place due to air compression when the air chamber of the second model is sealed from atmosphere. The technique described for monochromatic waves. Results obtained from the testing of an OWC are presented. Spectral methods are applied to the technique, and then implemented to measure the parameters of the model OWC. This allows multiple frequencies to be analysed using a single set of tests.**

***Index Terms*—Oscillating water column, air compressibility, hydrodynamic parameters, tank tests, spectral analysis.**

I. Introduction

As part of ongoing efforts to develop a floating, multiple-OWC combined wind/wave energy platform, a numerical model of a single, fixed OWC was implemented as described in [1]. The hydrodynamic parameters required for the numerical model were obtained from the boundary element method solver WAMIT [2]. Comparisons between the predictions made by the numerical model, with the results obtained from narrow tank testing of a physical OWC, found good agreement for some incident wave conditions, while for other wave conditions the agreement was poor.

A separate investigation using the physical model described in [1] into the effect of air compressibility on the behaviour of small-scale physical models of OWC devices was undertaken. This model is referred to as 'Model 1' herein. As discussed in, for example, [3] and [4], the effect of the compressibility of the air within an OWC device above the free surface can be linearised and modelled as a spring. However, when tank testing is performed at atmospheric pressure, the air spring effect does not scale correctly if the air volume above the free surface of the water column is scaled in accordance with Froude scaling i.e. the cube of the scaling factor. One approach to including the effect of the air spring at small scale is to scale the air volume by the square of the scaling factor, while the wetted surface of the physical model remains scaled in accordance with Froude scaling. This approach was approximated in, for example, [5]. As part of the investigation into the effect of air compressibility that led to the current work, a second physical model of the OWC was constructed. The volume of air above the water column for Model 1 used in [1] was scaled geometrically, whereas the volume of air in the chamber of the second model, referred to as 'Model 2' herein, was scaled by the square of the scaling factor.

The approach to measuring the hydrodynamic parameters of an OWC proposed in the current work uses the wave maker of a wave tank to excite the water column during fixed-body oscillation tests, which are performed on Model 1. During fixed-body tests, the air chamber above the water column is sealed from atmosphere. As the volume of air is small and almost incompressible, the water column may be considered fixed during fixed-body tests. Forced-oscillation tests are performed on Model 2. As for the fixed-body tests, the air chamber is sealed from atmosphere, and the wave maker is used to excite the water column. Due to the compressibility of the large volume of air contained within the enlarged air chamber of Model 2, motion of the water column will occur. The need for a separate forcing rig when physically measuring the hydrodynamic parameters of the OWC is thus eliminated.

In this work, the novel approach to measuring the hydrodynamics for an OWC is first described for monochromatic waves. The proposed method is then extended to make use of spectral methods using polychromatic waves. Preliminary results of the implementation of the method in both monochromatic and polychromatic waves are presented. Finally, a second variant of forced-oscillation testing, which eliminates the need for the enlarged air box, is proposed.

II. Determining Hydrodynamic Parameters using Monochromatic Waves

For a fixed, single OWC operating in the pumping mode, the equation of motion in the frequency domain for the water column, under the assumption of linear conditions, is given by:

$$Fe_7(\omega) = \left[C_{77} - \omega^2 \left(M_7 + A_{77}(\omega)\right) + j\omega(B_{77}(\omega))\right] U_7 + \Delta P(\omega) \times A_{owc} \quad (1)$$

In Equation 1, $Fe_7(\omega)$ refers to the frequency-dependent exciting force acting on the water column due to the incident wave, M_7 refers to the mass of the water column, $A_{77}(\omega)$ refers to the frequency-dependent added mass of the water column in the pumping mode, $B_{77}(\omega)$ is the frequency-dependent radiation damping in the pumping mode, C_{77} refers to the hydrostatic stiffness of the water column, and U_7 represents the vertical displacement of the water column from the 'at rest' position, $\Delta P(\omega)$ refers to the difference in pressure between the air chamber and atmosphere, and A_{owc} is the cross-sectional area of the water column.

A method for experimentally measuring the hydrodynamic parameters of a rigid body is well established, see, for example, [6]. A fixed-body test is used to measure the exciting force acting on a body due to an incident wave. During a fixed-body test, a body is held fixed in a wave tank. The body is then subjected to incident waves, and the force acting on the body is measured using force transducers. A forced-oscillation test may be used to determine the added mass and radiation damping coefficients of a body. The body is driven about the still-water position in the absence of waves. The motion of the body is known, and the force acting on the body may be recorded. This information may be used to determine the added mass and radiation damping coefficients for the frequency of oscillation at which the test is performed. A forced-oscillation test to measure the added mass and radiation damping coefficients may be conducted for any frequency of interest by driving the body at that frequency.

Fixed-body and forced-oscillation tests may be adapted to measure the hydrodynamics of an OWC as described in, for example, [7] and [8]. When performing a fixed-body test on an OWC, the water column is held fixed by completely sealing the air chamber above it. The OWC is then subject to incident waves, and the exciting force may be determined by measuring the pressure in the air above the water column using a pressure transducer. In this case, Equation 1 reduces to:

$$Fe_7(\omega) = \Delta P(\omega) \times A_{owc} \quad (2)$$

A time series of the exciting force acting on the water column may be obtained by multiplying the time series of the gauge pressure measured in the chamber by the area of the water column. The exciting force may be transformed into the frequency domain using a Fourier transform. While some motion of the water column can occur due to the compressibility of the air above it, this effect is negligible at the model scales used here when the air chamber of the OWC is scaled geometrically [9]. Care must be taken to ensure the air chamber is fully sealed during fixed-body tests.

The method to measure the exciting force acting on the water column of Model 1 used herein is identical to that described in [7], and takes the form of a fixed-body test. As mentioned above, for Model 1 the wetted surface, and the volume of air above the water column in the OWC chamber, are Froude-scaled. Model 1 was installed in a wave tank. The air chamber above the water column was sealed, and the model was subject to monochromatic, incident waves of low amplitude to minimise non-linear effects. For each frequency of interest, a separate test was performed. For each test, the time series of the differential pressure in the air chamber was recorded. The pressure time series was converted to the exciting force time series using Equation 2, before being transformed into the frequency domain using a Fourier transform.

Typically, forced-oscillation tests are performed using a forced-oscillation rig which, for model OWCs, takes the form of an air hose connected to the air chamber which drives the water column through the application of positive and negative pressure. As for the fixed-body tests, the force acting on the water column would be measured using a pressure transducer, and the instantaneous free surface elevation of the water column would be measured using a wave probe located in the OWC chamber. From this information, the frequency-dependent added mass and radiation damping would then be determined. It is the forced-oscillation test proposed herein that differs from that used typically.

The forced-oscillation tests described herein were performed using Model 2. As mentioned above, Model 2 includes a large airbox above the water column constructed so that the volume of air within the airbox is reduced by the square of the scaling factor as proposed in [5]. This volume of air is sufficiently large to allow the water column to move due to air compression, even when the airbox is completely sealed from atmosphere. Model 2 is then subject to the same incident wave conditions to which Model 1 was subject during the fixed-body test. For Model 2, with reference to 1, $U_7 \neq 0$ as the water column may now move due to the compressibility of the large volume of air. In this case, Equation 1 does not reduce further. U_7 is recorded by a wave probe located at the centroid of the free surface of the water column. ΔP is also recorded, and then multiplied by A_{owc} in order to determine the force acting on the water column due to both the compression of air in the airbox in response to the motion of the water column and the exciting force due to the incident wave. In effect, the wave maker is being used to force-oscillate the water column. Both the force and displacement signals can be transformed into the frequency domain using Fourier transforms. With knowledge of the mass, M_7, and the coefficient of buoyancy, C_{77}, of the water column, which may be determined from the geometry of the water column, and using Fe_7, measured using the fixed-body method, the only remaining unknown terms in Equation 1 are A_{77} and B_{77}, which may be found for each frequency tested as follows:

$$A_{77} = \frac{C_{77} - \Re\left[\frac{Fe_7 - \Delta P \times A_{owc}}{U_7}\right]}{\omega^2} - M_7 \tag{3}$$

$$B_{77} = \frac{\Im\left[\frac{Fe_7 - \Delta P \times A_{owc}}{U_7}\right]}{\omega} \tag{4}$$

Equations 3 and 4 may be used to find the added mass and radiation damping for the water column once the phases between Fe_7 (as determined from the fixed-body tests on Model 1), U_7 and $\Delta P \times A_{owc}$ (as measured in the forced-oscillation tests on Model 2), are known.

III. Determining Hydrodynamic Parameters using Polychromatic Waves

System identification of linear systems may be performed based on spectral analysis as described in [10] and [11]. Using the method outlined in Section II, separate fixed-body and forced-oscillation tests must be performed for each frequency of interest in order to measure the hydrodynamic parameters at the corresponding frequency. However, in principle, the frequency-dependent parameters of a linear system can be identified from a single set of tests during which the system is excited by a random, stationary and ergodic input. The ratio between the input to a frequency-dependent linear system, and the output of the same system, is termed the frequency-dependent transfer function of the system. Spectral analysis allows for the determination of the transfer function for such a system when the system is excited by an input as described above, once both the input to, and output of, the system are known, for frequencies that are contained within the spectrum of the input signal. Ocean waves can be considered stationary and ergodic over the time scale of a few hours (see, for example, [12]), and the pseudo-random sea-states generated by the narrow tank are stationary and ergodic, once the system is run for a sufficiently long period of time. An OWC in which the water column moves in response to an incident wave can be considered a single-input/single-output (SISO) system, with the exciting force, Fe_7, as the input and the water column displacement, U_7, as the output. The frequency-dependent hydrodynamic parameters of the system may be found from the transfer function between Fe_7 and U_7. An SISO system can be represented graphically in the time domain and the frequency domain as shown in Figure 1.

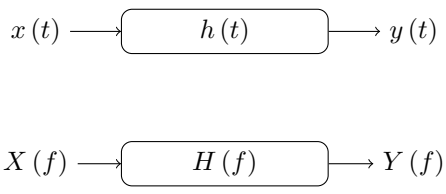

Fig. 1. A single-input/single-output system in the time domain and the frequency domain.

In Figure 1:

$x(t)$	represents the stationary input
$y(t)$	represents the output
$h(\tau)$	represents the impulse response of the system
$X(f)$	represents the Fourier transform of $x(t)$
$Y(f)$	represents the Fourier transform of $y(t)$
$H(f)$	is the frequency-dependent, Fourier transfer function between $X(f)$ and $Y(f)$

$H(f)$ is the Fourier transform of $h(\tau)$.

The two-sided, autospectral density function, $S_{xx}(f)$ for an input time signal $x(t)$ is related to the autospectral density function, $S_{xx}(f)$ for an output signal $y(t)$ by:

$$S_{yy}(f) = |H(f)|^2 S_{xx}(f) \tag{5}$$

Similarly, the two-sided, cross-spectral density function, $S_{xy}(f)$ of the two time signals, $x(t)$ and $y(t)$ are related by:

$$S_{xy}(f) = H(f) S_{xx}(f) \tag{6}$$

In Equations 5 and 6, the frequency may be either positive or negative, and both $S_{yy}(f)$ and $S_{yy}(f)$ are two-sided. In terms of one-sided spectral density functions, which are defined for positive frequencies only, 5 and 6 become:

$$G_{xy}(f) = H(f) G_{xx}(f) \tag{7}$$

$$G_{yy}(f) = |H(f)|^2 G_{xx}(f) \tag{8}$$

where:

$G_{xy}(f)$	is the one-sided cross power spectral density of $x(t)$ and $y(t)$
$G_{xx}(f)$	is the one-sided power spectral density of $x(t)$
$G_{yy}(f)$	is the one-sided power spectral density of $y(t)$

The frequency-dependent transfer function of an SISO system may thus be written:

$$H(f) = \frac{G_{xy}(f)}{G_{xx}(f)} \tag{9}$$

A full treatment of the theory underpinning spectral analysis may be found in, for example, [10]. Spectral analysis may be used to determine the frequency-dependent hydrodynamic parameters of an OWC based on Equation 1. Equation 1 may be recast into the form of an SISO system as follows:

$$\begin{aligned}&[Fe_7(f) - \Delta P(f) \times A_{owc}] = \\ &\left[C_{77} - \omega^2 (M_{77} + A_{77}(f)) + j\omega B_{77}(f)\right] U_7(f)\end{aligned} \tag{10}$$

The SISO in Equation 10 may be represented graphically as shown in Figure 2.

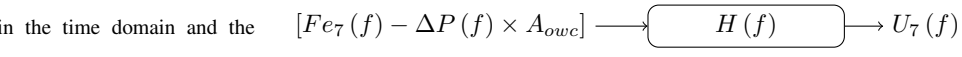

Fig. 2. The SISO system representation of the relationship between $[Fe_7(f) - \Delta P(f) \times A_{owc}]$ and $U_7(f)$ for a single-chamber OWC.

In Figure 2, $H(f)$ is the Fourier transfer function between $[Fe_7(\omega) - \Delta P(\omega) \times A_{owc}]$ and $U_7(\omega)$. Equations 3 and 4 may then be recast in terms of $H(f)$ and used to determine the added mass and radiation damping for each frequency component in $[Fe_7(\omega) - \Delta P(\omega) \times A_{owc}]$ as follows:

$$\Re\{H(f)\} = C_{77} - \omega^2 (M_{77} + A_{77}(f)) \tag{11}$$

$$\Im\{H(f)\} = \omega B_{77}(f) \tag{12}$$

and hence:

$$B_{77}(f) = \frac{\Im\{H(f)\}}{\omega} \tag{13}$$

$$A_{77}(f) = \frac{C_{77} - \Re\{H(f)\}}{\omega^2} - M_{77} \tag{14}$$

Note that herein, $Fe_7(f)$ was obtained from a fixed-body test using Model 1, while $\Delta P(f)$ and $U_7(f)$ were obtained from a forced-oscillation test using Model 2.

Equations 13 and 14 can be used to determine the hydrodynamic parameters of an OWC once $Fe_7(t)$, $\Delta P(t)$ and $U_7(t)$ can be measured. It is also possible to experimentally determine the frequency-dependent transfer function between U_7 and η, where η is the wave elevation at the centroid of the water column. η may be determined by measuring the free surface elevation in the tank in the absence of the OWC model, at the point where the centroid of the water column would be.

Note that, in order to demonstrate the validity of applying spectral methods to the determination of hydrodynamic parameters, the authors carried out a preliminary investigation into this approach. In that study, spectral methods were used to recover the hydrodynamic parameters of a cylinder from the simulated motions of the cylinder in response to a polychromatic input. The hydrodynamic parameters used to create the simulation were obtained from WAMIT, and were successfully recovered from the simulated results for the cylinder using the methods described above.

IV. Experimental Method

In this section, the method by which the theory described in Sections II and III was implemented to measure the hydrodynamic parameters of the OWC described in [1] is described for both mono- and polychromatic waves.

A. Monochromatic Technique

1) Fixed-body Test: Model 1 was first installed in the narrow tank, and the air chamber above the water column was carefully sealed using silicone. The airtight seal was verified by subjecting the model to large regular waves. Leak spray was used to locate any air escaping from the air chamber, and any leaks were then sealed, again using silicone. This process was repeated as necessary to ensure the air chamber was completely sealed from the surrounding atmosphere.

Fixed-body tests were then performed for wave frequencies of 0.4 Hz to 1.2 Hz, in increments of 0.05 Hz. These tests were run for wave amplitudes of 5 mm, 10 mm and 15 mm, so that the effect of non-linearities, such as viscous damping, could be observed. Thus, a total of 51 frequency/amplitude pairings were examined.

During the fixed-body tests, the variation in pressure within the air chamber, the motions of the water column and the free surface elevation at a point up-wave of the OWC chamber were recorded, using a sampling rate of 128 Hz. This relatively high sampling rate was used to allow the results of multiple tests be aligned, as described below. Data was recorded once steady-state conditions had been reached for all tests. Figure 3 illustrates a schematic of the fixed-body test set-up.

During the tests, the signal from the wave probe located in the chamber can be monitored visually to ensure no movement of the water column takes place, and to confirm not only that the chamber remains airtight, but also to confirm the small volume of air within the chamber is effectively incompressible.

2) Forced-oscillation Test: Once the fixed-body tests were completed, Model 1 was removed from the tank, and Model 2 was installed in the tank. Care was taken to ensure that Model 2 was positioned so that the location of the water column relative to the wave maker was identical to that for Model 1 during the fixed-body tests. A custom-made locator jig was constructed for this purpose. Care was also taken to ensure that the up-wave wave probe remained in the same location relative to both the wave maker and the water column. Model 2 was now subject to the identical tests to which Model 1 was subject during the fixed-body tests, while the same signals were recorded at the same sampling rate. Figure 4 illustrates a schematic of Model 2 installed in the narrow tank.

The results obtained from the fixed-body tests, using Model 1, and the forced-oscillation tests, using Model 2, were then combined to determine the hydrodynamic parameters of the water column. The purpose of the measurements obtained using the wave probe located up-wave of the OWC model is to allow the results from a fixed-body and a forced-oscillation test of the same amplitude/frequency pairing to be aligned. The location of this wave probe may be seen in Figures 3 and 4. Once the up-wave probe remains in the same location relative to the wave maker and the water column for a pair of fixed-body and forced-oscillation tests, the time series of the wave elevation at the location of the wave probe may be used to align the phases of the results from the two separate tests.

A number of methods to align data sets were explored, including the cross-correlation of the signals, or using the Hilbert transform of the signals. A third method, a fast Fourier transform (FFT) technique, described below, was selected, as FFTs are also required elsewhere by the technique to determine the hydrodynamics of the OWC. An FFT is performed on the free surface elevation time series data from the up-wave probe for the fixed-body test. By selecting the frequency bin with the greatest amplitude in the resultant transform, the magnitude and phase of the dominant frequency within the time series is found. These correspond to the magnitude and frequency

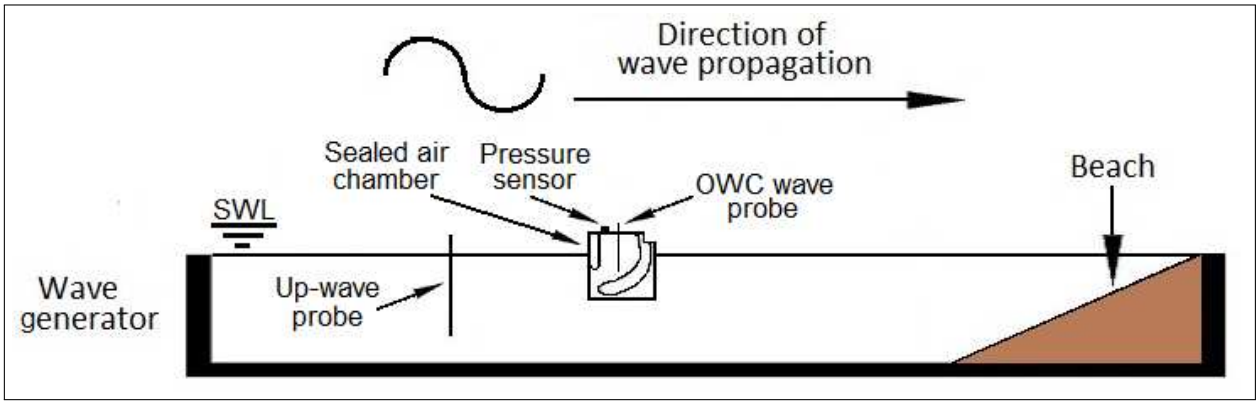

Fig. 3. Schematic of Model 1 installed in the narrow tank at DkIT.

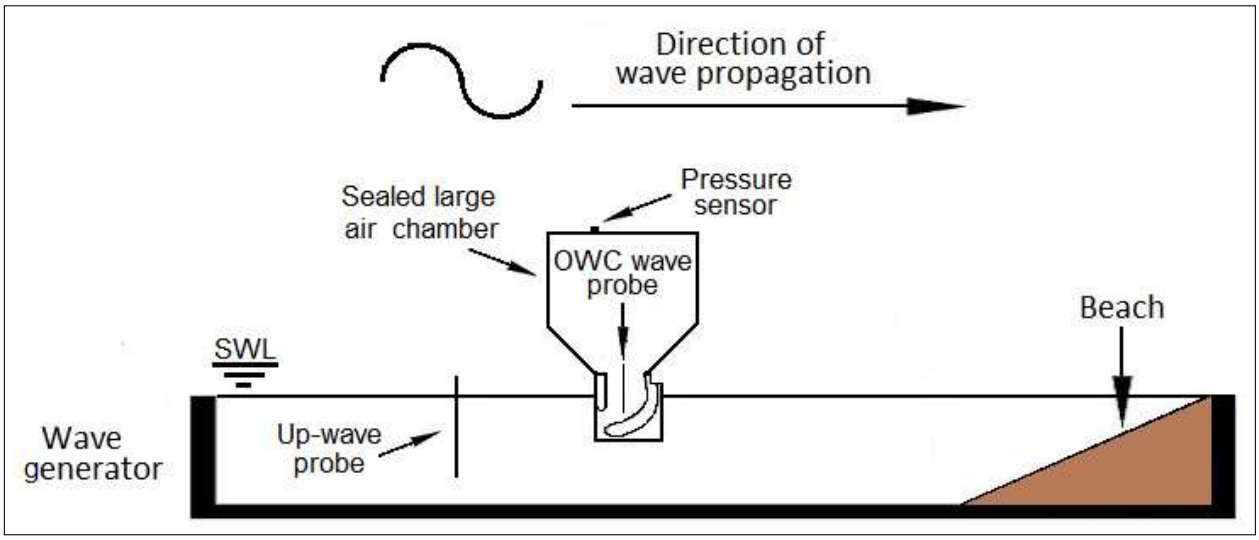

Fig. 4. Schematic of Model 2 installed in the narrow tank at DkIT.

of the incident wave during the fixed-body test. Likewise, an FFT is performed on the up-wave free surface elevation for the forced-oscillation test, and the magnitude and frequency of the incident wave during the forced-oscillation test found. The angle between the up-wave free surface elevation during the fixed-body test, and the corresponding signal during the forced-oscillation test, may now be found, once the frequency of the incident wave is known. Terming this angle β, the time offset between the phases of the incident wave during the fixed-body test and the incident wave during the forced-oscillation test may now be found using Equation 15:

$$\text{Time Offset} = \frac{\beta \times \text{ Wave Frequency}}{2\pi} \tag{15}$$

Data from the forced-oscillation test is then offset by the appropriate number of time steps so that the phase of the incident wave for both the fixed-body and forced-oscillation tests are equal. The data obtained from both tests can now be considered temporally aligned, and Equations 3 and 4 may be used to determine the hydrodynamic parameters of the OWC.

B. Polychromatic Technique

The method by which the hydrodynamic parameters were measured using spectral techniques also requires a fixed-body test, performed using Model 1, and a forced-oscillation test, performed using Model 2. First, however, it was necessary to ensure that the narrow tank at DkIT is capable of repeatably generating the same polychromatic waves as input to the separate tests.

1) Tank Repeatability: In order to investigate if the tank is capable of reproducing a pseudo-random wave elevation time series, a Bretschneider spectrum with $Te = 0.85$ s and $Hs = 0.03$ m was created. The wave maker was used to generate the Bretschneider spectrum for three hours with no model installed, and the free surface elevation recorded at a point midway between the wave maker and the beach. The spectrum was run three times to create three time series of the free surface elevation at the same point in the tank. Figure 5 illustrates a Bretschneider spectrum with the wave spectrum with $Te = 0.85$ s and $Hs = 0.03$ m, and the power density spectrum of the time series of the free surface elevation recorded during one of the three-hour test runs when no model

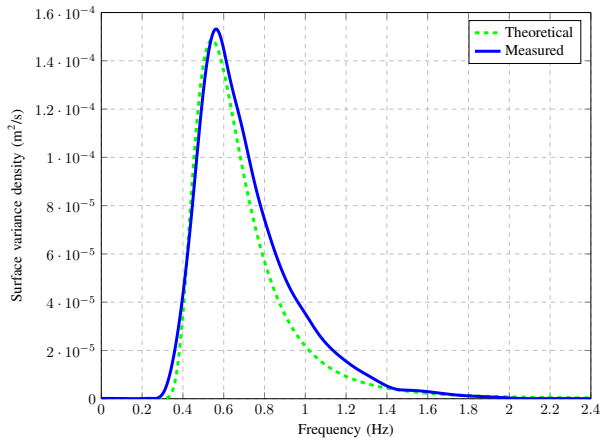

Fig. 5. Bretschneider spectrum used to verify repeatability of pseudo-random wave generation of the narrow tank at DkIT.

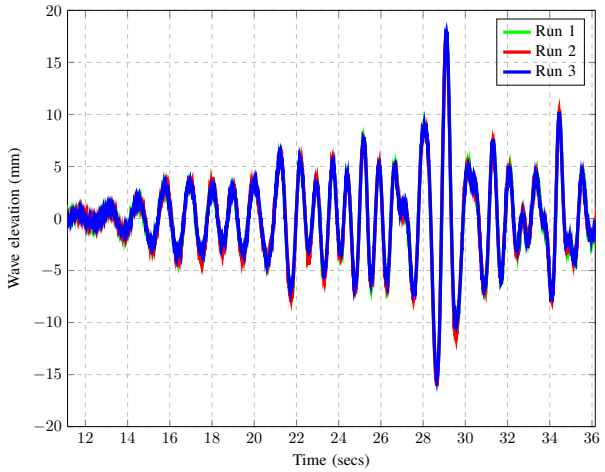

Fig. 6. Three time series of free surface elevation in the narrow tank.

was installed in the tank.

The cross-correlation function was used to find the best fit between the time series measured by the wave probe midway between the wave maker and the beach for the length of the three series, and two of the time series were offset as appropriate so as to temporally align the signals. A sample of the aligned signals is illustrated in Figure 6.

Once aligned, two measures were used to assess the repeatability of the signal: the cross-correlation factor and the root mean square (RMS) of the signal. The cross-correlation factor between each pair of three-hour signals is calculated. A value of 1 indicates a total positive correlation, a value of -1 indicates a total negative correlation and 0 indicates no correlation [13]. Table I lists the cross-correlation factor between all possible pairings of the three signals. The correlation factor between the first and the second time series of free surface elevation is termed X_{12}, the correlation factor between the first and the third time series of free surface elevation is termed X_{13}, and the correlation factor between the second and the third time series of free surface elevation is termed X_{23}.

TABLE I
CROSS-CORRELATION FACTOR BETWEEN THREE TIME SERIES IN THE NARROW TANK.

Cross-correlation Factor		
X_{12}	X_{13}	X_{23}
0.9976	0.9955	0.9964

As can be seen, there is a very high level of correlation between the three signals, in excess of 99%, and this could possibly be improved further with a higher sampling rate allowing for more precise alignment of the signals. However, the cross-correlation factor alone is insufficient to ensure the wave spectrum generated by the narrow tank is repeatable. Consider a time series, $y_1 = x(t)$, and a second time series which comprises of the first scaled by a linear factor, $y_2 = Ax(t)$, where A is the linear factor. The cross-correlation between y_1 and y_2, $X_{y_1 Y_2} = 1$. The high cross-correlations in Table I demonstrate that the shapes of the times series of the free surface elevation for the three tests are very similar, but are not necessarily the same magnitude. To check that the magnitude of the free surface elevation is also repeatable, the RMS value of the free surface elevation recorded in the three tests was calculated, and the results are presented in Table II.

TABLE II
RMS OF THE WAVE ELEVATION RECORDED DURING THREE TIME SERIES IN THE NARROW TANK.

RMS of wave elevation		
Run 1	Run 2	Run 3
5.3090 mm	5.3104 mm	5.2082 mm

As can be seen, the RMS value of the wave elevation remains consistent throughout the three tests. Note that while the position of the wave probe used to create the results shown in Table II was not altered, the probe was re-calibrated between the second and third sets of measurements, which may explain the slight difference in the RMS value for the third run when compared to the first two. Based on the cross-correlation factor and the RMS value, it can be seen that the tank is capable of repeatedly generating pseudo-random wave elevations at different times.

A fixed-body test was conducted in which Model 1 was subject to an incident wave spectrum shown in Figure 5. Model 2 was then installed in the tank so that the location of the water column matched that as for Model 1 during the fixed-body test, and a forced-oscillation test was performed using the identical spectrum. The results from the two tests were temporally aligned using the initial time series of the up-wave probe, before reflected or radiation waves from the model begin to manifest at the up-wave probe location, from the two tests. The two time series were cross-correlated to find the temporal offset between the wave maker starting and the beginning of data recording. This offset was then used to align

the data sets so that the measurements between tests might be considered as 'simultaneous'.

V. Results

In this section, the results obtain for the hydrodynamic parameters of the model OWC measured, as described above, are presented.

A. Monochromatic Results

The magnitude of the frequency-dependent exciting force acting on the water column, determined using Equation 2, is shown in Figure 7. The exciting force values have been normalised by the wave amplitude so that the results for 5 mm, 10 mm and 15 mm waves can be directly compared.

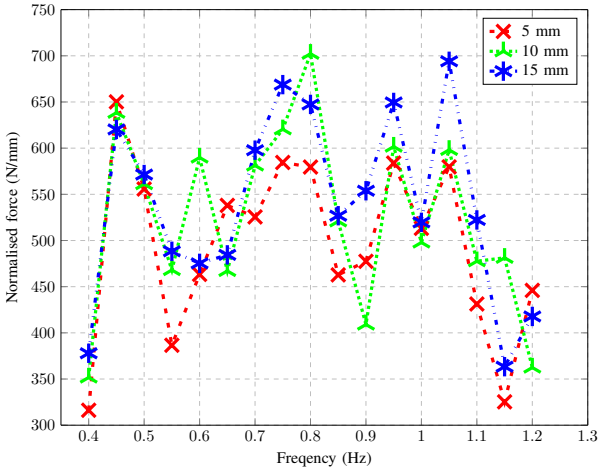

Fig. 7. Variation in normalised exciting force vs. frequency.

Figure 8 illustrates the frequency-dependent added mass for the OWC found by implementing Equation 3, while Figure 9 illustrates the frequency-dependent radiation damping found by implementing Equation 4 for the three amplitudes used during the monochromatic tests.

B. Polychromatic Results

The results obtained for the added mass and radiation damping for the model OWC from the polychromatic tests using Equations 13 and 14 are shown in Figures 10 and 11.

VI. Discussion

The results obtained using the method proposed for measuring the hydrodynamics of an OWC suggest that the method has potential, but also raise some issues which could be investigated further in future work. Consider first the added mass results obtained using the methods described in Sections II and III. As can be seen in Figure 8, for monochromatic waves, a strong level of consistency has been obtained between the added mass results determined for the three different incident wave amplitudes used across the range of wave frequencies. Furthermore, close agreement has also been obtained for the added mass determined using both monochromatic and

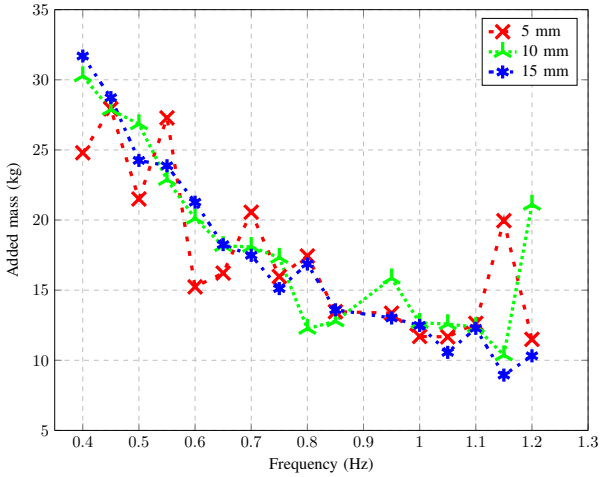

Fig. 8. Variation in added mass vs. frequency.

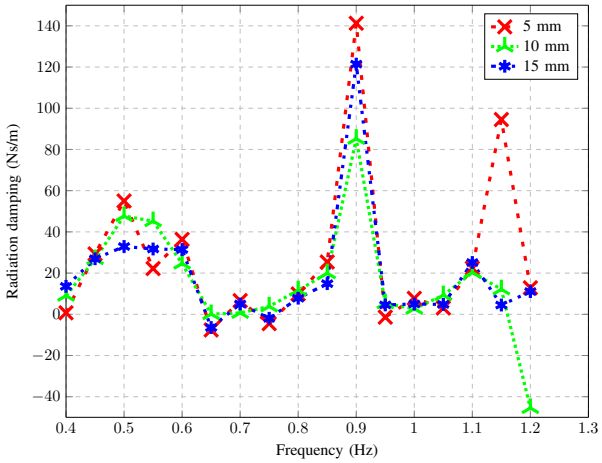

Fig. 9. Variation in radiation damping vs. frequency.

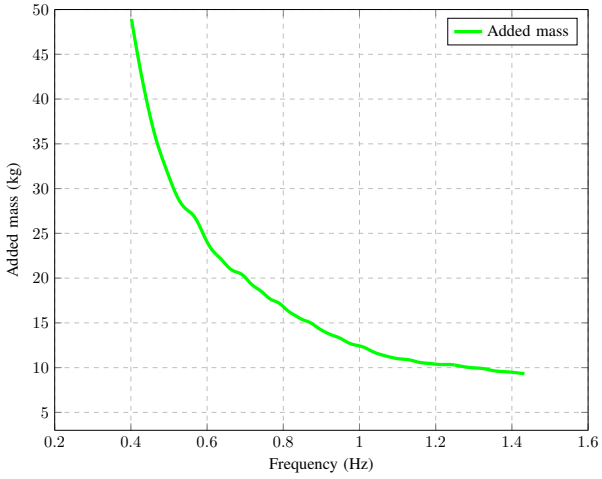

Fig. 10. Added mass vs. frequency for single-chamber OWC using spectral analysis.

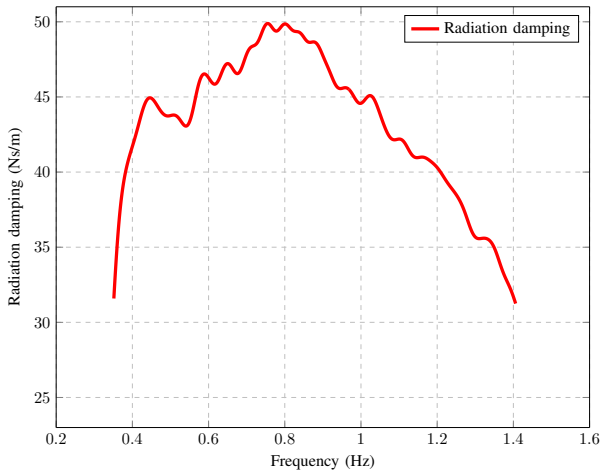

Fig. 11. Radiation damping vs. frequency for single-chamber OWC using spectral analysis.

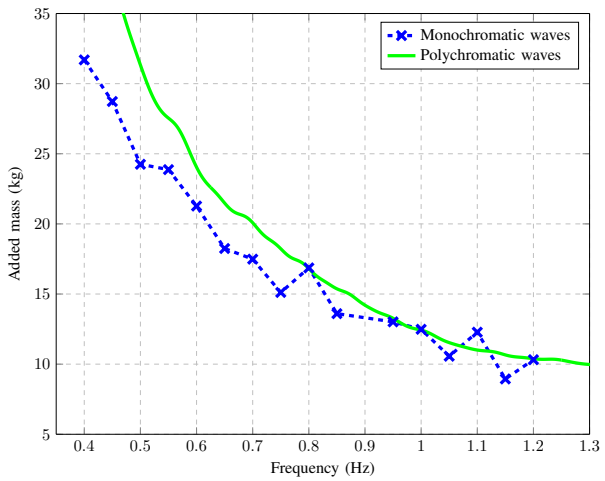

Fig. 12. Comparison between the added mass for a single OWC determined using mono- and polychromatic waves, as described in Sections II and III.

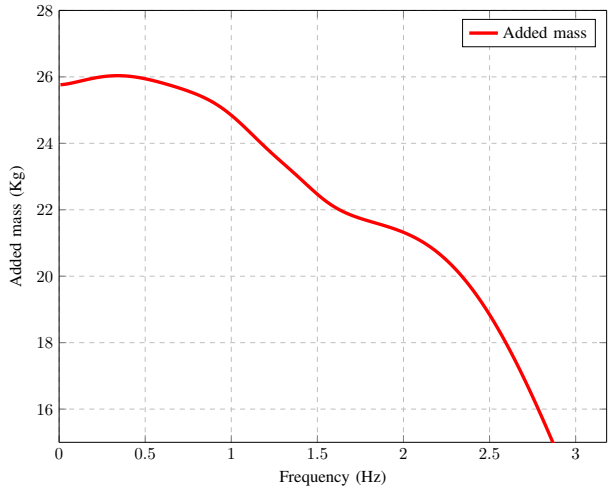

Fig. 13. Frequency-dependent added mass calculated by WAMIT.

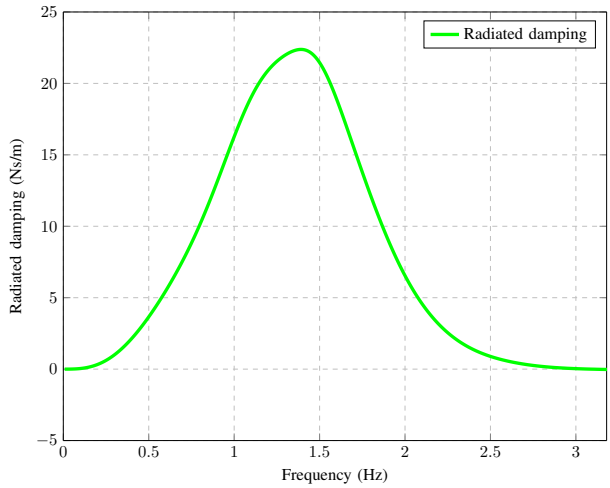

Fig. 14. Frequency-dependent radiation damping calculated by WAMIT.

polychromatic waves, as can been seen in Figure 12, where the results for the added mass as measured using monochromatic waves with an amplitude of 15 mm are overlaid on the added mass as measured using polychromatic waves.

This consistency in the added mass results would suggest that the proposed measuring technique has merit. The added mass and radiation damping results for the OWC obtained using the numerical software tool WAMIT [2], which are described in [1], are shown in Figures 13 and 14. Comparing the added mass values obtained numerically and the values obtained experimentally herein shows that while the form of the added mass versus frequency curves obtained numerically and experimentally do not agree, the magnitudes of the experimental results are of the expected order.

The results illustrated in Figure 9 for the radiation damping found using monochromatic waves show good agreement between the different amplitudes of incident wave used to perform the tests, suggesting that the motions involved were not sufficient for viscous damping to have a significant effect. Also, an outlier is clearly seen for each amplitude at 0.9 Hz. Furthermore, the radiation damping curves in Figure 9 dip below zero, which is not realistic. Figure 15 compares the results obtained for the radiation damping using mono- and polychromatic waves. Note that the outlier at 0.9 Hz, which is not present in the polychromatic waves, has been removed from the monochromatic example in this figure. As is the case for the added mass, the order of magnitude for the radiation damping values obtained numerically and experimentally are the same. However, the agreement between the results obtained using monochromatic waves and those using polychromatic waves is not strong. Nonetheless, once the outlier has been removed, the radiation damping results obtained using monochromatic waves do have the expected form of a radiation damping curve, with a peak damping between 0.5 Hz and 0.6 Hz. A number of possible explanations

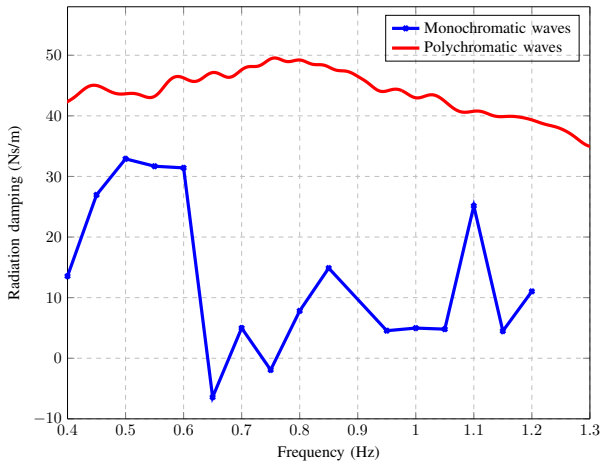

Fig. 15. Comparison between the radiation damping determined using mono- and polychromatic waves.

for the anomaly at 0.9 Hz, and for the difference in the radiation damping results for the mono- and polychromatic waves, are suggested below.

A. Issues with the Process for Measuring the Hydrodynamics of an OWC

There are a number of possible explanations for the outliers that occur, and for the discrepancy between some of the results presented in this paper. First is the assumption that the OWC moves only in a piston-like fashion, analogous to a heaving body. This neglects sloshing modes. However, such modes are present. During the testing that was performed using Model 2, a camera trained on the water surface was installed in the air box, which clearly showed the presence of sloshing modes in the motion of the water column, which were particularly pronounced at the higher frequencies used during the testing. Such sloshing will obviously manifest on the readings from the wave probe located within the OWC chamber and call into question the assumption that the wave probe located at the centroid of the water column surface is measuring only the heave mode of the water column at high frequencies. Furthermore, given the curved geometry of the OWC used herein (which can be seen in Figures 3 and 4), run-up of the incident wave on the curved surface of the back wall of the chamber is likely exacerbating the sloshing modes.

Potential sources for error may also have arisen when Model 1 was replaced in the tank with Model 2. Every caution was taken to ensure the water columns were positioned identically in the tank, and that the location of the internal wave probes within the chambers was the same. However, slight positioning differences can effect the outcome of the analysis, particularly given how small the phase difference between signals, such as the pressure signal for the fixed-body tests and the equivalent signal during the forced-oscillation tests, can be. Related to this is the need to temporally align data from different tests. The potential for error here is clear, and the best fit can only be achieved to a precision of one sample time step.

Another possible source of error is that it is not known how effective the narrow tank paddle is at absorbing wave reflections, in particular those at higher frequencies. Previous work has shown that the beach in the narrow tank at DkIT is effective in absorbing waves, and that, when no other obstruction is present in the tank, the wave maker is calibrated to accurately generate the waves requested. However, for high frequency waves, where the energy in the wave is located towards the top of the water column, much of this energy can be reflected back towards the wave maker by a model in the tank. If the wave maker is not effectively removing this reflected energy, the energy may be partially reflected back again towards the model by the wave maker. This reflected energy may thus potentially interfere with the incident wave as experienced by the model.

These issues suggest ways in which the process for measuring the hydrodynamics of an OWC might be improved in the absence of a dedicated forced-oscillation rig, and further follow up work that could be carried out on the topic. Firstly, to address the issue of sloshing within the OWC chamber, the process could be perfected using a simple, box-like OWC designed so as to minimise run-up over the range of frequencies of interest. For such an OWC, the assumption that the water column acts in a piston-like mode only would be more valid. Once the process was perfected for a single-mode water column, it could potentially be developed further to include sloshing modes. The use of multiple wave probes to record the motion of the water column at several points within the chamber in the direction of wave travel would allow the motion of the free surface to be better captured, and the different sloshing modes of the water column could be decomposed from the time series measured by the multiple wave probes.

To explore whether waves are being reflected from the wave maker during a test, experiments could be performed in a large, 3-dimensional tank. Such a setting would minimise the effect of any wave energy reflected, rather than absorbed, by the wave maker, although different results would be expected for the hydrodynamics in the 3-dimensional case when compared to the 2-dimensional case [14].

The ability of the wave maker to create virtually identical free surface elevation time series has been demonstrated. Thus, the need to align data sets could be eliminated if the same action used to start the wave maker was also used to start the data acquisition system, which is not currently implemented at the DkIT narrow tank, where the wave maker and data acquisition system are currently entirely isolated from each other. A system to begin recording at the same moment the wave maker is initiated would seem a sensible improvement to the current setup.

It has been noted that the phase difference between some signals, notably the pressure signals obtained during the fixed- and forced-oscillation tests, is small, and thus any error in measurement would have a large effect on the results obtained for the hydrodynamics. However, if confidence can be had in one or other of the added mass or radiation damping, the other could be found using the Ogilvie Relations [15] derived

from the Kramers-Kronig Transform or the Hilbert Transform [16], in a process similar to that used to reconstruct the added mass from the radiation damping for the numerical model, as described in [1].

B. Future Work

The relationship between the pressure drop across an orifice, and the volumetric and mass flow rate of air through the orifice is not linear [17]. When an OWC with an orifice is acted on by a monochromatic incident wave, the variation of air pressure within the OWC chamber does not vary linearly with respect to time. For Equation 1 to be valid, it must be possible to transform all parameters into the frequency domain, that is to say, all parameters must vary linearly with time. It is for this reason that the forced-oscillations test were performed using Model 2, since by introducing a large volume of air which is sealed from the atmosphere above the water column, motion of the water column in response to an incident wave can occur, while the air pressure in the large air volume above the water column will vary linearly.

However, it is possible to configure an OWC so that the pressure varies linearly while still allowing airflow into and out of the chamber, if the OWC may be linearly damped. The non-linear variation in air pressure within an OWC chamber fitted with an orifice can be understood as a consequence of the non-linear mass flow of air through the orifice. However, it is possible to allow airflow between the chamber and atmosphere, and hence allow water column motion for for Model 1 in response to an incident wave, while also producing close to linear pressure variations within the chamber. Linear air pressure variation with water column motion can be achieved by covering an orifice with a permeable membrane. Such an approach has been used in previous work to model the damping characteristics of a Wells Turbine on an OWC, and carpet tiles are one form of permeable membrane that have been used [18]. Future work may investigate the implementation of a forced-oscillation test as described in Sections II and III on an OWC fitted with a permeable membrane. Should it prove possible to induce linear pressure variations in air trapped within the OWC chamber, the results thus obtained may then be transformed into the frequency domain. The results obtained could then be used to determine the hydrodynamic parameters of an OWC without the need for an additional large airbox as used herein.

Another possible avenue of investigation is to use the admittance approach to modelling an OWC based on susceptance and conductance as described in [19]. The fixed-body test would be replaced by a fully-open, undamped OWC, although sloshing could be a significant issue with this approach, which has not been explored at this time.

ACKNOWLEDGMENTS

The authors wish to acknowledge the Carpentry and Joinery Department of DkIT for their assistance in the construction of the marine plywood model used during the narrow tank testing described herein, and Wave Energy Ireland Ltd. and the Sustainable Energy Authority of Ireland for providing funding for this research under Grant No. OCN/00031.

REFERENCES

[1] T. Kelly, T. Dooley, J. Campbell, and J. Ringwood, "Efforts towards a validated time-domain model of an oscillating water column with control components," *Proceedings of the 11th European Wave and Tidal Energy Conference*, 2015.

[2] WAMIT Inc., *WAMIT User Manual Version 7.0*. MA USA: WAMIT Inc., 2012, vol. 1.

[3] R. Jefferys and T. Whittaker, *Latching Control of an Oscillating Water Column Device with Air Compressibility*. Berlin, Heidelberg: Springer Berlin Heidelberg, 1986, pp. 281–291.

[4] J. Weber, "Representation of non-linear aero-thermodynamic effects during small scale physical modelling of OWC WECs," in *Proceedings of the 4th International Conference on Ocean Energy*, October 2012.

[5] A. F. Falcão and J. C. Henriques, "Model-prototype similarity of oscillating-water-column wave energy converters," *International Journal of Marine Energy*, vol. 6, pp. 18–34, 2014.

[6] J. Journee and W. Massie, *Offshore Hydrodynamics*. Delft University of Technology, 2001.

[7] T. P. Stewart, "The influence of harbour geometry on the performance of oscillating water column wave power converters," Ph.D. dissertation, The Queen's University of Belfast, 1993.

[8] A. Aalbers, "The water motions in a moonpool," *Ocean Engineering*, vol. 11, no. 6, pp. 557–579, 1984.

[9] B. Massey and J. Ward-Smith, *Mechanics of Fluids*. CRC Press:London, UK, 1998.

[10] J. Bendat and A. Piersol, *Engineering Applications of Correlation and Spectral Analysis*. Wiley, 1980.

[11] ——, *Random Data: Analysis and Measurement Procedures*, ser. Wiley Series in Probability and Statistics. Wiley, 2011.

[12] S. Chakrabarti, *Hydrodynamics of Offshore Structures*. Computational Mechanics Springer-Verlag, 1987.

[13] D. Sheskin, *Handbook of Parametric and Nonparametric Statistical Procedures*, 3rd ed. CRC Press, 2003.

[14] N. Newman, "The exciting forces on fixed bodies in waves," *Journal of Ship Research*, vol. 6, no. 3, pp. 423–433, 1963.

[15] T. Ogilvie, "Recent progress towards the understanding and prediction of ship motions." in *6th Symposium on Naval Hydrodynamics*, 1964.

[16] F. King, *Hilbert Transforms*, ser. Encyclopedia of Mathematics and its Applications. Cambridge University Press, 2009.

[17] "Measurement of fluid flow by means of pressure differential devices inserted in circular cross-section conduits running full - Part 2: Orifice plates." International Organization for Standardization, Geneva, CH, Standard, Mar. 2003.

[18] Y. Delaure and A. Lewis, "3D hydrodynamic modelling of fixed oscillating water column wave power plant by a boundary element methods," *Ocean Engineering*, vol. 30, no. 3, pp. 309–330, 2003.

[19] J. Falnes and P. McIver, "Surface wave interactions with systems of oscillating bodies and pressure distributions," *Applied Ocean Research*, vol. 7, no. 4, pp. 225–234, 1985.